URSI AP-RASC 2019, New Delhi, India; 09 - 15 March 2019

Nonalcoholic Fatty Liver Texture Characterization based on Transfer Deep Scattering Convolution Network and Ensemble Subspace KNN classifier

R Bharath and P Rajalakshmi
WiNet Lab, Department of Electrical Engineering,
IIT Hyderabad, Telangana, India.

Abstract

Nonalcoholic Fatty Liver Disease (NAFLD) is highly prevalent and may progress to chronic diseases if left untreated. Early detection and diagnosis are crucial to prevent the complications associated with NAFLD. Fatty liver diagnosis is widely done through ultrasound scanning. Based on the density of fat, the liver is classified into four categories. The ultrasonic texture characteristics of liver parenchyma vary with the concentration of fat, and hence the radiographers use this as a property to classify the fatty liver. Classifying the nonalcoholic fatty liver is highly challenging to the radiographers due to the minute variations observed in the characteristics of the texture. To assist the radiographers in doing accurate diagnosis, we propose a novel computer-assisted novel algorithm based on compressed transfer scattering coefficients and ensemble subspace KNN classifier. The proposed algorithm classified the texture with an accuracy of 98.8% when tested on a data size of 1000 images, where each category consists of 250 images each.

1 Introduction

Excess deposits of fat in the liver also known as Nonalcoholic Fatty Liver Disease (NAFLD) is the major cause for chronic diseases such as cirrhosis, fibrosis, liver cancer, etc. From recent studies, it is found that 40% of the population in developed countries and 20 to 30% population in developing countries are suffering from the NAFLD [1]. Depending on the density of fatty granules, the fatty liver is characterized into four categories namely normal, mild, moderate and severe respectively. In general, patients suffering from normal and mild fatty liver does not need medication and is easily reversible, while the patients suffering from moderate and severe fatty liver needs medical attention to prevent further complications associated with the disease. The texture of liver parenchyma correspond to different grades of fatty liver is shown in Figure 1, these textures are cropped at the regions of liver parenchyma. The textures of normal liver appear like flakes with coarser and rugged. As the concentration of fat increases, the coarseness of the texture reduces and becomes finer and finer. The difference inferred across the texture of different grades of fatty liver is minute, and hence it is very challenging for the radiographers to classify the fatty content. A study says that the radiographers have low mean intra and inter agreement of 76% and 72% respectively in classifying normal and fatty liver, while it is 47 to 59% and 59 to 64% respectively in classifying between mild, moderate and severe fatty liver [2].

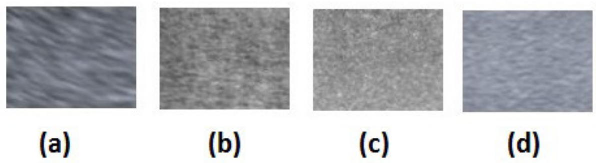

Figure 1. Textures correspond to (a) normal (b) mild (c) moderate (d) severe

A plethora of work has been reported regarding the computer-aided diagnostic algorithms for fatty liver classification, but not much focus is laid on quantifying the different grades of the fatty liver [3]. Determining the exact fatty content in the liver is very crucial in many cases. For example in liver transplantation, there is a high probability that receptor will suffer from liver failure if the donor has a mild fatty liver. There is a high chance that the patient who undergoes liver resections will suffer from postoperative complications. Under the circumstances, there is a need for computer-aided diagnostic algorithms to accurately quantify the fatty content in the liver. In [4], we have proposed a classification algorithm based on scattering coefficients with cubic support vector machine (SVM) classifier, where we achieved an accuracy of 96.6% in classifying the different grades of fatty liver. In this paper, we present an extension of [4], where we obtained a better accuracy with compressed transfer scattering coefficients with ensemble subspace KNN classifier. Scattering Coefficients (SC) gives the stable and translational invariant representations and also preserves the high-frequency information which is useful for classification [5]. Ensemble subspace K nearest neighbor classifier is used for classifying the texture based on the SC's features.

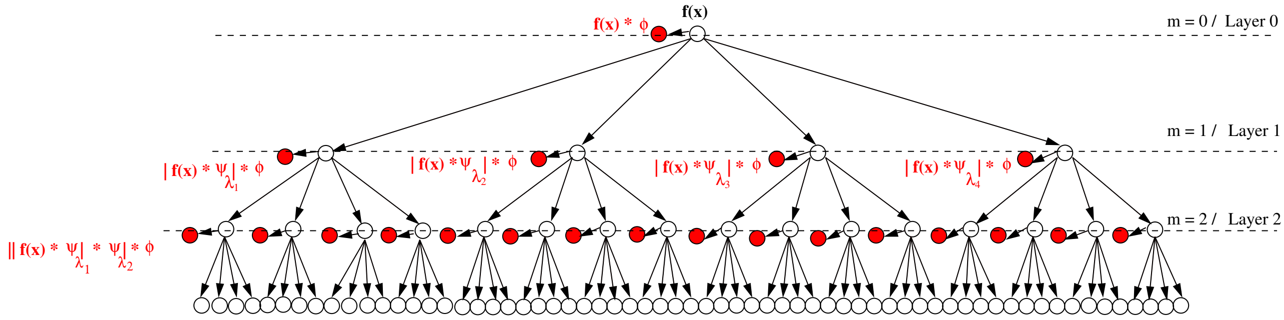

Figure 2. Architecture of ISCN. The red bubbles represents SC's, * indicates the convolution operator and m defines the depth of the network.

2 Transfer Scattering Network based Fatty liver Texture Classification.

The SC's are computed using an Invariant Scattering Convolution Network (ISCN) architecture [5]. The invariant representations of SC's are obtained by progressively cascading wavelet transform with modulus and averaging operators. The computation of SC's using ISCN is shown in Figure 2. The red bubble indicates the SC's while the white bubble indicates the propagator signal $|.|$ on which low pass filtering results in SC's. In the zeroth layer of a network, the image is convolved with a low pass scaling function ϕ defined as

$$Layer\ 0,\ S_x(0) : f(x) \star \phi_{2^J}, \tag{1}$$

where $f(x)$ represent an image, $\phi(x)_{2^J} = 2^{-2J}\phi(2^{-J}x)$ represent Gaussian low pass filter, J denotes the largest scale space variable and $\star$ denotes the convolution operation.

In the first layer, a low pass filter is convolved with the modulus of the complex wavelet transform of an image

$$Layer\ 1,\ S_x(\lambda)\ : \mid f(x) \star \psi_\lambda \mid \star \phi_{2^J}, \tag{2}$$

where $\psi_\lambda(x) = 2^{-2j}\psi(2^{-j}r_\theta x)$ represent all the dilated and rotated versions of the band pass wavelets with $\lambda = (2^j, \theta)$, $0 \leq j_1 < j_2 < \cdots < j_s < \cdots < j_t < \cdots < J$, j is denotes scale space variable, and r_θ represent group of rotations computed as θ: $2\pi l/L$, where $0 \leq l <$ L. The $f \star \psi_\lambda$ computes gradient of an image at different directions and scales capturing high frequency. Since high frequency is the source of variability, modulus operator is applied on $f(x) \star \psi$ to obtain an envelope of the signal which is equivalent to a low pass signal thus reducing the variability in the signal. Additionally, modulus operator avoids the wavelet coefficients leading to zero while averaging which result in loss of information. The coefficients of $\mid f(x) \star \psi \mid$ may still loose information due to singularities i.e., $\mid f(x) \star \psi \mid = 0$ which is prevented by choosing a complex wavelet of the form

$$\psi = \psi_a + i\psi_b, \tag{3}$$

where ψ_a and ψ_b denotes real and imaginary parts of the complex wavelet. The modulus operator on complex wavelet is computed by

$$\mid \psi \mid = (\psi_a^2 + \psi_b^2)^{1/2}. \tag{4}$$

The translation invariance is obtained by averaging the modulus of complex wavelet coefficients. The averaging operation i.e., convolution of ϕ_{2^J} with $\mid f(x) \star \psi \mid$ will result in a shift invariance $f(x) = f(x-t)$ where $|t| < 2^J$.

The SC's of the second layer is obtained as

$$Layer\ 2,\ S_x(\lambda_1, \lambda_2)\ : \mid f(x) \star \psi_{\lambda_1} \mid \star \psi_{\lambda_2} \mid \star \phi_{2^J}, \tag{5}$$

where ψ_{λ_1} corresponds to all scales and rotations, while ψ_{λ_2} corresponds only to the scales $j_t > j_s$, since, the second order interference coefficients are negligible for $j_t < j_s$. The coefficients obtained in the second layer extracts co-occurrence information of the image at two scales 2^{j_1} and 2^{j_2} corresponding to two different orientations θ, which interpreted as a interaction coefficients hence called as SC.

The high discriminative nature of the SC's can be obtained with higher depths. The discriminative nature of SC's corresponding to the texture of four classes of fatty liver is visualized as the disk covering the entire frequency support of image as shown in Figure 3. We can observe that SC's gives discriminative features both in the first and second layer for all the four classes of NAFLD. For four scales and eight orientations and for the network depth of two the invariant scattering convolution network gives a total of 417 SC matrices. If the image is of dimension $[M,N]$, then the SC's obtained at each node is of dimension $[M/2^{J-1}, N/2^{J-1}]$. For the image of size $[78,100]$ and for scale $J = 4$, the SC's are of the dimension $[10,13]$. Each coefficient is locally invariant to a width of eight pixels. The SC's are of high dimension, and if we use all these coefficients as features, the classification algorithm will suffer from the curse of dimensionality. To obtain the compact representation from SC's and to achieve global invariance to translations, the SC's in each index is summed and considered as a single feature.

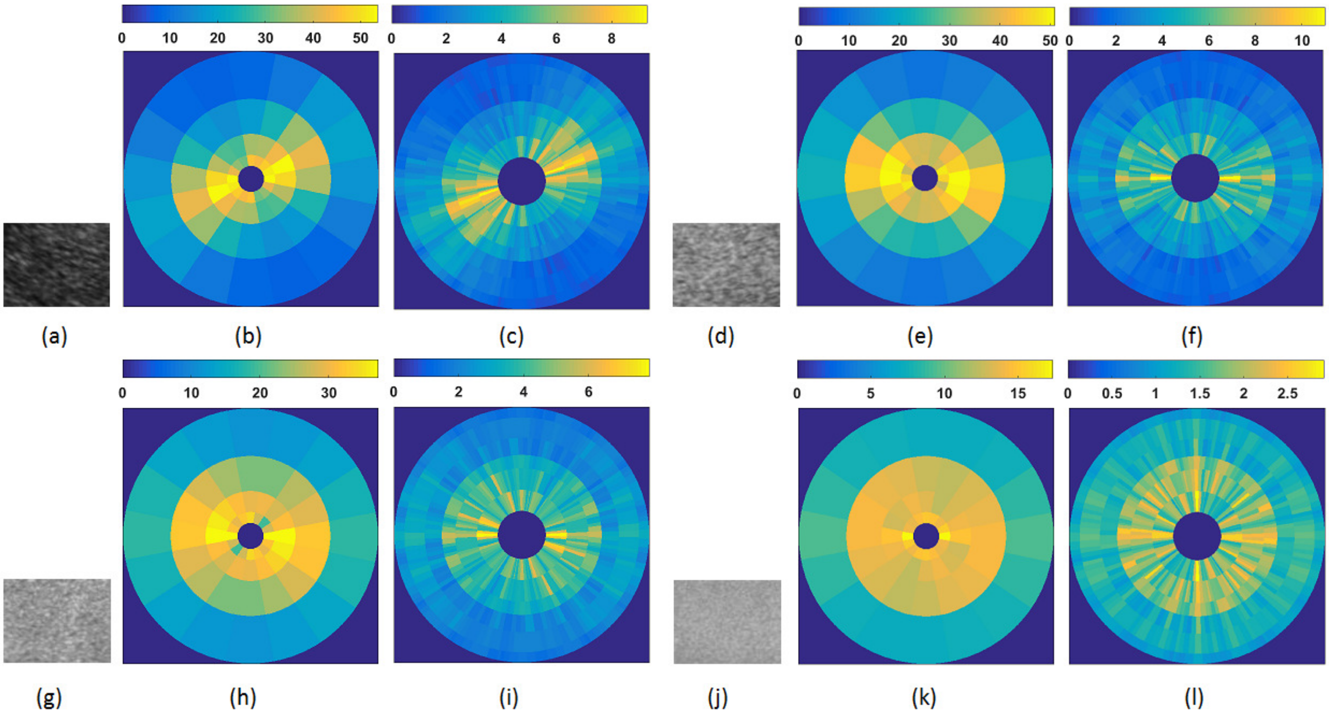

Figure 3. Visual difference observed in SC's (4 scales and 8 orientations) for different grades of fatty liver. (a), (d), (g), (j) Texture images of of normal, mild, moderate and severe fatty liver respectively. (b), (e), (h), (k) First layer SC's of normal, mild, moderate and severe fatty respectively. (c), (f), (i), (l) Second layer SC's of normal, mild, moderate and severe fatty respectively.

The SC's obtained after the second layer is embedded with information about the SC's from where it is propagated from the previous layers. The efficacy of the features extracted from ISCN in classification lies in extracting the representations which are not present in previous layers. To decorrelate the redundant information present in deeper layers, the SC's are normalized by dividing children node $S_x(\lambda_1, \lambda_2)$ with corresponding parent node $S_x(\lambda_1)$. The efficiency of SC features is evaluated with EKNN classifier. In EKNN classifier, instead of using a single classifier, multiple KNN classifiers with a subspace of features per classifier have been used in classification. The optimal number of classifiers, the number of features per classifier and the number of nearest neighbors used for each classifier are determined by cross-validation.

3 Results

The images are acquired using Siemens ultrasound scanner with phased array transducer from Asian Institute of Gastroenterology Hyderabad. The dataset consists of 1000 texture images where each image category consists of 250 image texture patches. The texture patches are cropped from the liver parenchyma, and ensured that the image patches is homogeneous and free from the blood nodules, periportal veins, etc. Each texture image is of size 78 x 100. Ten-fold cross-validation scheme is employed to test the proposed algorithm. The optimal architecture for achieving maximum classification accuracy have to be obtained empirically. The accuracy of compressed transfer SC with EKNN classifier with respect to orientations and scales is shown in Table. 1. In the experiments, the number of learners in EKNN classifier is fixed to 30, the number of features for each classifier is taken half of the feature size and number of nearest neighbours as 5. The maximum classification accuracy of 98.2% is achieved at four scales and eight orientations. By optimal tuning of the parameters of EKNN classifier, the classification accuracy is further improved. The optimal parameters of EKNN classifier are computed using the ten-fold cross-validation. The optimal parameters are obtained at K=5 nearest neighbors, the number of randomly selected features at 93 and number of classifiers at 63.

The performance of the proposed feature extraction scheme with some of the popularly used texture features in representing the liver ultrasonic texture is shown in Table. 2. The performance of the features is evaluated with KNN, cubic SVM and EKNN classifier. The proposed transfer SC features with EKNN classifier has performed better than the texture features used in the literature for representing the ultrasonic texture of liver. SC's performed better when compared to other texture features, since the SC's extract the sufficient gradient information with respect to different scales and orientations, and have the provision to extract as many features as possible which is needed for classification.

The confusion matrix for the proposed algorithm is shown in Table. 3, moderate fatty liver classified with an accuracy

Table 1. Accuracy(%) of the transfer based SC features for different scales and orientations with EKNN classifier, depth of the network $m = 2$ and size of the image 78×100. Features from all the layers are concatenated as a single feature vector and used in classification. For EKNN classifier, number of learners is fixed to 30, subspace dimension of features is taken half of feature size.

	Orientations						
Scales	2	3	4	5	6	7	8
2	88.1	90.1	91.4	90.9	92.2	93.3	94.8
3	91.0	93.0	95.5	94.9	96.5	96.9	97.4
4	92.9	94.6	95.2	96.2	96.9	98.0	98.2
5	93.3	95.4	96.1	96.5	97.6	96.9	97.8
6	94.6	95.5	95.9	96.2	96.1	95.6	96.2

Table 2. Performance of the popularly used texture features in grading the fatty liver.

Features	**KNN**	**SVM**	**EKNN**
GLCM [6]	86.7	92.3	91.4
GLRLM [6]	85.8	92.4	90.4
Laws [7]	82.9	88.5	91.6
GIST [8]	80.8	90.1	88.7
Wavelet_Energy [9]	87.5	90.4	88.2
Gabor_Energy [9]	87.4	92.8	91.1
Transfer SC features	94.0	96.5	98.8

of 100%, while the severe fatty liver classified with an accuracy of 99.6%, while the normal and mild texture classified with an accuracy of 98.8% and 96.8% respectively. Considering the normal textures as negative images and mild, moderate and severe as positive images, the proposed algorithm classified the nonalcoholic fatty liver texture with a sensitivity of 98.8% (741 out of 750 images with fatty liver identified correctly) and specificity of 98.8% (247 out of 250 images with normal liver identified correctly). It is also observed that no images of moderate and severe are misclassified as normal and mild which is the significant advantage from the proposed algorithm since the risk associated in classifying the diseased case as normal is high.

4 Conclusion

In this paper, we proposed a novel compressed transfer SC based features for classifying the textures correspond to NAFLD. The proposed feature extraction scheme proved very effective in representing the texture of fatty liver which replicated in achieving good classification accuracy. The proposed algorithm can assist the radiographers to quantify the fatty content in the liver, and it can also be used to assist the semi-skilled persons in remote areas to diagnose the patients.

Table 3. Confusion matrix for the SC features extracted for computed for a network depth $m = 2$ with EKNN classifier.

	Predicted Class			
True Class	normal	mild	moderate	severe
normal (250)	247	2	1	0
mild (250)	2	242	5	1
moderate (250)	0	0	250	0
severe (250)	0	0	1	249

5 Acknowledgements

The authors are thankful to Dr. Mohammad Abdul Mateen, Radiologist AIG, Hyderabad, India, for providing the annotated database.

References

[1] Bellentani, Stefano, Federica Scaglioni, Mariano Marino, and Giorgio Bedogni "Epidemiology of non-alcoholic fatty liver disease." Digestive diseases, 28.1, 155-161, 2010.

[2] Strauss S, Gavish E, Gottlieb P, Katsnelson L. "Interobserver and intraobserver variability in the sonographic assessment of fatty liver." Am J Roentgenol, vol. 189.6, pp:320-323, 2007.

[3] Goceri, Evgin, Zarine K. Shah, Rick Layman, Xia Jiang, and Metin N. Gurcan "Quantification of liver fat: A comprehensive review." Computers in biology and medicine, 71, 174-189, 2016.

[4] R Bharath, and P Rajalakshmi. "Deep scattering convolution network based features for ultrasonic fatty liver tissue characterization." In Engineering in Medicine and Biology Society (EMBC), pp. 1982-1985, 2017.

[5] Bruna, Joan, and Stphane Mallat. "Invariant scattering convolution networks." IEEE transactions on pattern analysis and machine intelligence, vol. 35.8, pp:1872-1886, 2013.

[6] Wu, Cheng-Chi, Wen-Li Lee, Yung-Chang Chen, and Kai-Sheng Hsieh "Evolution-based hierarchical feature fusion for ultrasonic liver tissue characterization." IEEE journal of biomedical and health informatics, vol.17.5 967-976, 2013.

[7] Wu C-M, Chen Y-C, Hsieh K-S. "Texture features for classification of ultrasonic liver images." IEEE Trans Med Imaging, vol. 11.2, pp.141-52, 1992.

[8] Oliva A, Torralba A. Modeling the shape of the scene: a holistic representation of the spatial envelope. Int J Comput Vis, vol. 2.3, pp.145-75, 2001.

[9] Lee, Wen-Li et al. "Ultrasonic liver tissues classification by fractal feature vector based on M-band wavelet transform." IEEE Transactions on Medical Imaging, vol. 22.3, pp: 382-392, 2003.